Hydrate inhibition in propylene glycol and glycerol systems

Proceedings of the 8th International Conference on Gas Hydrates (ICGH8-2014),
Beijing, China, 28 July - 1 August, 2014

HYDRATE INHIBITION IN PROPYLENE GLYCOL AND GLYCEROL SYSTEMS

Antonin Chapoy*, Rod Burgass, Bahman Tohidi
Hydrates, Flow Assurance & Phase Equilibria Research Group, Institute of Petroleum Engineering, Heriot-Watt University, Edinburgh EH14 4AS, Scotland, UK

ABSTRACT

In this communication, we report new experimental dissociation data for various systems consisting of methane at propylene glycol and glycerol concentration up to 50 wt%. The hydrate dissociation measurements were conducted using standard constant volume (isochoric) technique together with step-heating for achieving equilibrium conditions. A statistical thermodynamic approach, with the Cubic-Plus-Association equation of state, is employed to model the phase equilibria. The hydrate-forming conditions are modelled by the solid solution theory of van der Waals and Platteeuw. A good agreement between predictions and experimental data is observed, supporting the reliability of the developed model.

Keywords: Gas hydrate, equation of state, methane, propylene glycol, glycerol, experimental data.

NOMENCLATURE

a	Attractive parameter of the EoS
b	Co volume parameter of the EoS
BIP	Binary interaction parameter
C	Langmuir constant
CPA	Cubic Plus Association
EoS	Equation of State
f	Fugacity
g	Gas / Radial distribution function in the CPA EoS/ Constant
MEG	Monoethylene glycol
P	Pressure [MPa]
PG	Propylene glycol
R	Universal gas constant
SAFT	Statistical Associated Fluid Theory
SRK	Soave-Redlich-Kwong equation of state
sI	Structure-I
sII	Structure-II
T	Temperature [K]
V	Volume
$\bar{v}$	Number of cavities per water molecule in the unit cell
X	Mole fraction of molecules that are not-bonded to the site

Superscript

H	Hydrate
L	Liquid state
m	Cavity type
Ref	Reference property
V	Vapour state

Subscripts

0	Reference property
exp	Experimental property
i, j	Molecular species
HC	Hydrocarbon component
W	Water

Greek

α	Kihara hard-core radius
β	Refer to empty hydrate lattice
Δ	Association strength in the CPA EoS
ε	Kihara energy parameter
θ	Occupancy of the cavity
k	Boltzmann's Constant
ρ	molar density
σ	Kihara collision diameter
$\Delta C'_{pw}$	Heat capacity difference between the empty hydrate lattice and liquid water
$\Delta\mu^{\circ}_{w}$	Chemical potential difference between

* Corresponding author: Phone: +44(0)1314 513797 Fax +44(0)1314 513 797 E-mail: antonin.chapoy@pet.hw.ac.uk

	the empty hydrate lattice and ice at ice point and zero pressure
ω	The spherically symmetric cell potential in the cavity

INTRODUCTION

The economic risks involved in the development of offshore and deep-water reservoirs demand cost effective methods and techniques for providing flow assurance solutions. In offshore drilling, the pressure of the drilling fluid combined with relatively low seabed temperatures, can provide suitable thermodynamic conditions for the formation of gas hydrates in the event of a kick. This can cause serious well safety and control problems during the containment of the kick. For deepwater drilling, classical fluid (saturated saline solutions) may not provide the required protection unless combined with chemical inhibitors. The reported experimental data on gas hydrate formation in drilling fluids is very limited, and in some cases inconsistent.

Propylene glycol (PG) and glycerol are often present in the formulation of the drilling fluid. Propylene glycol has also been suggested as an alternative to monoethylene glycol (MEG). PG shares many of the properties of MEG in terms of freezing point depression, however MEG is toxic. Conversely, PG is a food additive which is not harmful to humans.

Accurate knowledge of gas hydrate dissociation conditions and phase behaviour of aqueous solutions of PG and glycerol is therefore crucial to avoid gas hydrate formation and for safe and economical design/operation of pipelines and production/processing facilities.

In this work, the statistical model uses the cubic-plus-association equation of state (CPA EoS) for fugacity calculations in all phases [1]. The hydrate-forming conditions are modelled by the solid solution theory of van der Waals and Platteeuw [2]. The performance of the model has been tested by comparing the predictions with the data generated in this laboratory as well as the most reliable data from the open literature for hydrate stability zone.

EXPERIMENTAL

Clathrate dissociation PT conditions were determined by standard constant volume cell isochoric equilibrium step-heating techniques. This method, which is based upon the direct detection (from pressure) of bulk density changes occurring during phase transitions, produces very reliable, repeatable phase equilibrium measurements [3].

Materials

Methane was purchased from BOC gases with a certified purity greater than 99.995 vol. %. PG and glycerol used in experiments were 99.5%+ pure, supplied by Sigma-Aldrich. Aqueous solutions were prepared using deionized water throughout the experimental work.

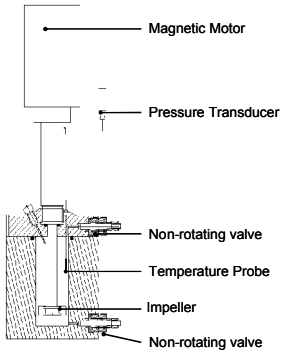

Figure 1 Schematic illustration of the autoclave cell used for PVT hydrate equilibrium studies

Experimental Apparatus

Figure 1 shows the apparatus used to determine the phase equilibrium conditions. The phase equilibrium is achieved in a cylindrical cell made of Hastelloy C276. The cell volume is about 80 ml and can be operated at pressures up to 700 bar between -77 and 50 °C. The equilibrium cell is immersed in a constant temperature liquid bath (Lauda Proline AP1290). The cryostat is capable of maintaining the cell temperature to within 0.02 °C. A platinum resistance probe monitors the temperature and is connected directly to a computer for direct acquisition. The pressure is measured by means of a Quartzdyne pressure transducer mounted directly on the cell and connected to the same data acquisition unit. This system allows real time readings and storage of temperatures and pressures throughout the different isochoric runs. To achieve a fast thermodynamic equilibrium and to provide a good mixing of the fluids, a high pressure magnetic stirrer (Top Industrie S.A − wetted parts made of Hastelloy C276) was used to agitate the test fluids at around 1,000 RPM with a Rushton type impeller. The calibration of the pressure transducer was checked regularly using a dead weight tester. The

pressure transducer is accurate to less than ±0.05 bar. The temperature probe was calibrated against a Prema 3040 precision thermometer. The uncertainty on temperature measurements is estimated to be better than ±0.1 °C.

THERMODYNAMIC MODELLING

A general phase equilibrium model based on the uniformity of component fugacities in all phases is used to predict the water activity and the hydrate suppression temperature of aqueous solutions of salt and alcohol. A description of the thermodynamic model can be found elsewhere [1, 4, 5, 6].

In summary, the statistical thermodynamics model uses the Cubic Plus equation of state for fugacity calculations in all fluid phases. The CPA EoS combines the well known Soave-Redlich-Kwong (SRK) EoS (Soave, 1972 [7]) for describing the physical interactions with the Wertheim's first-order perturbation theory (1987) [8], which can be applied to different types of hydrogen-bonding compounds. The parameters for pure water, PG and glycerol (associating compounds) in the CPA EoS have been determined by Kontogeorgis et al. (1999) [9], Derawi et al. (2003) [10] and Oliveira et al. (2009) [11], respectively. The 4C scheme has been selected for these 3 components. The CPA-EoS in terms of pressure P is given by:

$$P = \frac{RT}{V_m - b} - \frac{a(T)}{V_m(V_m + b)} - \frac{1}{2}\frac{RT}{V_m}\left(1 + \rho\frac{\partial \ln(g)}{\partial \rho}\right)\sum_i x_i \sum_{A_i}\left(1 - X^{A_i}\right) \quad (1)$$

where the physical term is that of the SRK EoS and the association term is taken from the SAFT EoS [11], x_i is the mole fraction of the component i and is the mole fraction of molecule i not bonded to the site A which is rigorously related to the association strength. Both depend on the structure of the molecule and the number and type of sites. The site fraction, X^{Ai} is related to the association strength between the site A on a molecule i, the site B on a molecule j, Δ^{AiBj} and the fractions X_B of all other kind of association sites B by:

$$X^{A_i} = \frac{1}{1 + \rho\sum_j n_j \sum_{B_i} X^{B_i}\Delta^{A_iB_i}} \quad (2)$$

where ρ is the molar density of the fluid, x_j is the mole fraction of substance j, X^{Ai} is related to the association strength between site A and site B on the molecule, and Δ^{AiBj}, the association strength, is the key quantity in the CPA EoS. Both X^{Ai} and Δ^{AiBj} depend on the structure of the molecule and the number and type of sites. The association strength between site A on molecule i and site B on molecule j is given by:

$$\Delta^{A_iB_j} = g(d)^{simp.}\left[\exp\left(\frac{\varepsilon^{AB}}{RT}\right) - 1\right]\beta^{A_iB_j} b \quad (3)$$

where $g(d)^{simp.}$ is the simplified expression of the radial distribution function as suggested by Kontogeorgis et al. (1999) [9], b is the co–volume parameter from the cubic part of the model, β and ε are the association volume and energy parameters of CPA, respectively. The latter two could be obtained from spectroscopy data but are in most cases estimated along with the parameters of the physical term using vapour pressure and density of pure compounds. The simplified expression of the radial distribution function is:

$$g(d)^{simp.} = \frac{1}{1 - 1.9\eta} \quad (4)$$

where η is the reduced fluid density given as:

$$\eta = \frac{1}{4} b\rho = \frac{b}{4V_m} \quad (5)$$

where ρ is the fluid density and the co–volume parameter, b, is assumed to be temperature independent, in agreement with most published equations of state.

The CPA model has five pure compound parameters; three for non-associating compounds (a_o, b and C_1) and two for additional parameters for associating compounds (ε^{AiBj} and β^{AiBj}). The CPA EoS parameters for the association compound used in this work are listed in Table 1.

CPA parameters for inert compounds considered in analogy with the van der Waals EoS, a and b are calculated from critical point conditions. In order to have an accurate representation of vapour pressures of pure compounds a temperature dependence of the attractive term through the Mathias & Copeman alpha function [12] is chosen:

$$a = \frac{\Omega_a R^2 T_c^2}{P_c} \quad (6)$$

$$b = \frac{\Omega_b R T_c}{P_c} \quad (7)$$

$$\Omega_a = 0.66121 - 0.76105 Z_c \quad (8)$$

$$\Omega_b = 0.02207 + 0.20868 Z_c \quad (9)$$

where Z_c is the critical compressibility factor, and ω is the acentric factor.

$$a(T) = \left[\begin{array}{l} 1 + C_1\left(1 - \sqrt{T_r}\right) \\ + C_2\left(1 - \sqrt{T_r}\right)^2 + C_3\left(1 - \sqrt{T_r}\right)^3 \end{array} \right]^2 \quad (10)$$

if $T > T_C$

$$a(T) = \left[1 + C_1\left(1 - \sqrt{T_r}\right)\right]^2 \quad (11)$$

The Mathias & Copeman alpha function parameters for the inert compounds, used in this work can be found in Coquelet et al., 2004 [13].

Comp.	a_0 (bar.L^2.mol^{-2})	b (L/mol)	C_1	ε (bar.L.mol^{-1})	β (x10^3)
Water [9]	1.228	0.01452	0.6736	166.55	69.2
PG [10]	13.836	0.0675	0.9372	174.42	19.0
Glycerol [11]	22.8	0.0706	1.18	140.36	25.0

Table 1. CPA Parameters for the associating compounds considered in this work

Modelling of hydrate phase

The hydrate-forming conditions are modelled by the solid solution theory of van der Waals and Platteeuw [2]. The statistical thermodynamic model of van der Waals and Platteeuw [2] provides a bridge between the microscopic properties of the clathrate hydrate structure and macroscopic thermodynamic properties, i.e., the phase behaviour. The hydrate phase is modelled by using the solid solution theory of van der Waals and Platteeuw [2], as implemented by Parrish and Prausnitz [14]. The fugacity of water in the hydrate phase is given by the following equation [15]:

$$f_w^H = f_w^\beta \exp\left(-\frac{\Delta\mu_w^{\beta-H}}{RT}\right) \quad (12)$$

where superscripts H and β refer to hydrate and empty hydrate lattice, respectively and μ stands for chemical potential. f_w^β is the fugacity of water in the empty hydrate lattice. $\Delta\mu_w^{\beta-H}$ is the chemical potential difference of water between the empty hydrate lattice, μ_w^β, and the hydrate phase, μ_w^H, which is obtained by the van der Waals and Platteeuw expression:

$$\Delta\mu_w^{\beta-H} = \mu_w^\beta - \mu_w^H = RT\sum_m \bar{v}_m \ln\left(1 + \sum_j C_{mj} f_j\right) \quad (13)$$

where $\bar{v}_m$ is the number of cavities of type m per water molecule in the unit cell, f_j is the fugacity of the gas component j. C_{mj} is the Langmuir constant, which accounts for the gas-water interaction in the cavity. The Langmuir constants are temperature dependent functions that describe the potential interaction between the encaged guest molecule and the water molecules surrounding it.

The mechanism of clathrate hydrate formation shows similarities to adsorption of molecules at sites on a surface. The assumptions made for the mechanism of Langmuir adsorption are also applicable for hydrate formation [2]. The occupancy of the sites on a surface in the Langmuir adsorption theory is given by a so-called Langmuir isotherm, which can also be developed for the occupancy of the cavities in clathrate hydrates.

$$\theta_{mj} = \frac{C_{mj} P_m}{1 + \sum_m C_{mj} P_m} \quad (14)$$

The Langmuir constant is a direct function of the particle partition function inside the cavity. The Langmuir constant is actually a description of the affinity of the empty cavity for a molecule to occupy this cavity; i.e., the higher the value for the Langmuir constant the more strongly the guest molecule will be encaged. If a potential guest molecule is too large to fit into the cavity, the Langmuir constant will have a value of zero. When the molecule is small related to the size of the cavity, the Langmuir constant also approaches zero. The relation for the Langmuir constant can be developed from the potential energy, and numerical values for the Langmuir constant can be calculated by choosing a model for the guest-host interaction [2]:

$$C_{mj}(T) = \frac{4\pi}{kT}\int_0^\infty \exp\left(-\frac{w(r)}{kT}\right) r^2 dr \quad (15)$$

where k is Boltzmann's constant. The function $w(r)$ is the spherically symmetric cell potential in the cavity, with r measured from the centre, and depends on the intermolecular potential function chosen for describing the encaged gas-water interaction. In the present work, Langmuir

constants have been calculated by both Kihara potential as well as direct techniques.

The Kihara potential function [17] is used as described in McKoy and Sinanoglu [18]. The Kihara potential parameters, α (the radius of the spherical molecular core), σ (the collision diameter), and ε (the characteristic energy) are taken from Tohidi-Kalorazi [19].

The fugacity of water in the empty hydrate lattice, f_w^{β} in Equation 12, can be calculated by:

$$f_w^{\beta} = f_w^{I/L} \exp\left(\frac{\Delta\mu_w^{\beta-I/L}}{RT}\right) \qquad (16)$$

where $f_w^{I/L}$ is the fugacity of pure ice or liquid water and $\Delta\mu_w^{\beta-I/LI}$ is the difference in the chemical potential between the empty hydrate lattice and pure liquid water. $\Delta\mu_w^{\beta-I/LI}$ is given by the following equation:

$$\frac{\Delta\mu_w^{\beta-I/L}}{RT} = \frac{\Delta\mu_w^{0}}{RT_0} - \int_{T_0}^{T} \frac{\Delta h_w^{\beta-I/L}}{RT^2} dT + \int_{0}^{P} \frac{\Delta v_w^{\beta-I/L}}{RT} dP \qquad (17)$$

where superscript *0* stands for reference property and *h* refers to molar enthalpy. $\Delta\mu_w^{0}$ is the reference chemical potential difference between water in the empty hydrate lattice and pure water at 273.15 K. $\Delta h_w^{\beta-I/L}$ and $\Delta v_w^{\beta-I/L}$ are the molar enthalpy and molar volume differences between an empty hydrate lattice and ice or liquid water. $\Delta h_w^{\beta-I/L}$ is given by the following equation [16, 20]:

$$\Delta h_w^{\beta-I/L} = \Delta h_w^{0} + \int_{T_0}^{T} \Delta C_{Pw}^{'} dT \qquad (18)$$

where *C'* and subscript *P* refer to molar heat capacity and pressure, respectively. Δh_w^{0} is the enthalpy difference between the empty hydrate lattice and pure water, at the ice point and zero pressure. The heat capacity difference between the empty hydrate lattice and the pure liquid water phase, $\Delta C_{Pw}^{'}$ is also temperature dependent and the equation recommended by Holder et al. [20] is used:

$$\Delta C_{Pw}^{'} = -37.32 + 0.179(T - T_0) \quad T > T_0 \qquad (49)$$

where $\Delta C_{Pw}^{'}$ is in $Jmol^{-1}K^{-1}$. Furthermore, the heat capacity difference between hydrate structures and ice is set to zero. The reference properties used can be found elsewhere [1].

RESULTS AND DISCUSSIONS

In this work, water activity at 25°C and atmospheric pressure for PG solutions have been measured by a reliable resistive electrolytic humidity sensor. Water activity, a_w, is defined as:

$$a_w(T,P) = \frac{f_w^{sample}(T,P)}{f_w(T,P)} \qquad (19)$$

Where f_w^{sample} and f_w are the fugacity of water in the sample and the fugacity of pure water, respectively. Water activities were measured using a Novasina Pro-Labmaster-aw (Novasina AS, Switzerland). As the water activity of a sample cannot be determined directly, this apparatus measures the partial water vapour pressure of a sample in a temperature-controlled environmental chamber and the water activity can be then derived from the following relation at low pressure:

$$a_w(T,P) \approx \frac{P_w^{sample}(T,P)}{P_w(T,P)} \qquad (20)$$

Where P_w^{sample} and P_w, are the partial water vapour pressure and the water vapour pressure, respectively. Samples were prepared, sealed in an air-tight container and allowed to equilibrate at 25°C. The water activities of the PG solutions are reported in Table 2 and used with freezing point data to tune the binary interaction parameters between PG and water. Freezing points and water activity after model optimization are plotted in Figures 2 and 3, respectively. The methane solubility data in PG of Galvao and Francesconi [1] were used to adjust the methane + PG k_{ij}. The optimum value is 0.25.

PG / wt%	a_w (±0.002)
10	0.973
20	0.916
25	0.922
30	0.908
40	0.861
50	0.802
60	0.727

Table 2. Experimental water activity PG solutions at 25°C

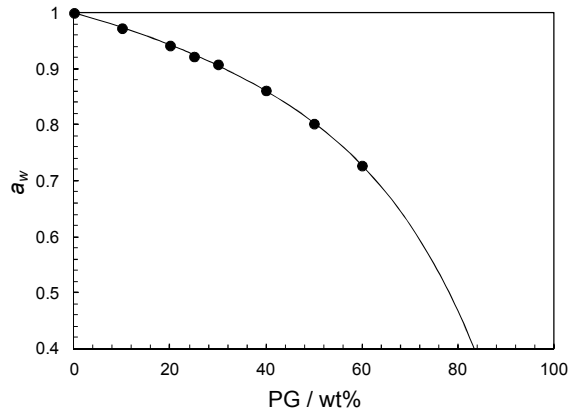

Figure 2 Experimental and calculated water activity of PG solutions at 25°C. ●: this work. Black curves: tuned model.

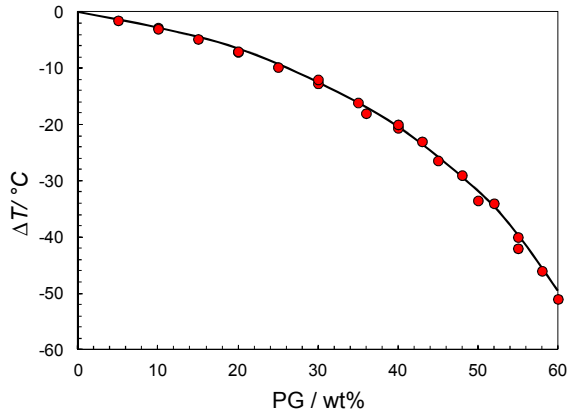

Figure 2 Experimental and calculated freezing point depression of PG solutions. ●: Literature data. Black curves: tuned model.

The new hydrate dissociation data generated for methane in the presence of aqueous PG solutions are listed in Table 3 and plotted in Figure 3. The results are in good agreement with the model predictions. Note that these new data were not used in fine-tuning the model predictions.

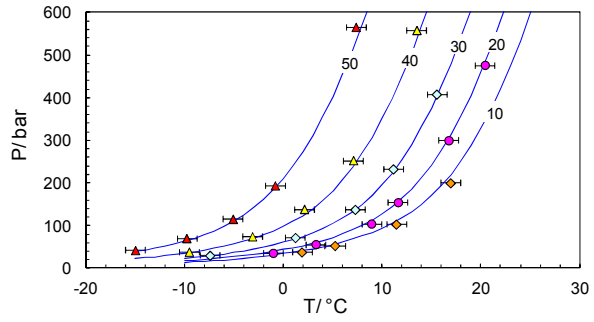

Figure 3 Experimental and predicted methane hydrate dissociation (sI) conditions in the presence PG (Model predictions are independent from experimental data) *(Error bars: ± 1 °C, only for visual purpose)*

PG		T / °C	P / bar
Mass %	Mol. %	(±0.1)	(±0.4)
10	2.6	1.85	38.0
		5.2	53.3
		11.4	103.4
		16.9	200.3
20	5.6	-1.05	36.1
		3.27	56.5
		8.9	104.7
		11.6	154.9
		16.72	300.2
30	9.2	-7.44	30.3
		1.2	72.1
		7.25	137.8
		11.1	232.8
		15.5	408.2
40	13.6	-9.55	38.9
		-3.15	74.8
		2.1	139.1
		7.07	253.5
		13.48	558.5
50	19.1	-15	42.7
		-9.8	70.7
		-5.1	115.8
		-0.85	194.4
		7.34	565.7

Table 3. Hydrate dissociation conditions in the Methane – Water + PG systems

Glycerol		T / °C	P / bar
Mass %	Mol. %	(±0.1)	(±0.4)
30	7.7	-1	45.1
		6.42	102.2
		11.7	205.1
		17.75	464.8
		20.35	627.4
40	11.5	-3.8	47.6
		3	104.5
		7.97	205.0
		11.2	332.9
		16.3	637.8
50	16.4	-6.7	64.3
		-0.3	138.5
		1.85	195.9
		5.96	373.7
		10.4	647.4

Table 4. Hydrate dissociation conditions in the Methane – Water + glycerol systems

A similar approach was used to tune the binary water +glycerol system(i.e. VLE data and freezing point data were used to optimize the model). Freezing points after model optimization are plotted in Figure 4.

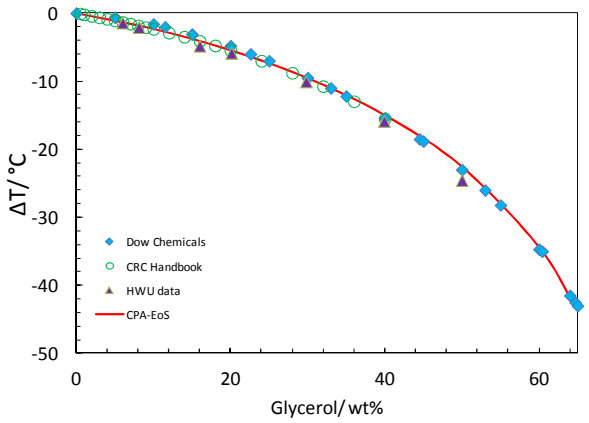

Figure 4 Experimental and calculated freezing point depression of glycerol solutions. Red curves: tuned model.

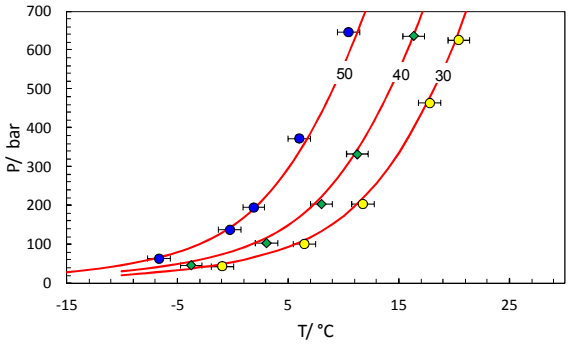

Figure 5 Experimental and predicted methane hydrate dissociation (sI) conditions in the presence glycerol (Model predictions are independent from experimental data) *(Error bars: ± 1 °C, only for visual purpose)*

Methane hydrate dissociation data measured in the present study are tabulated in Table 4. New experimental data for different concentrations of glycerol as a hydrate inhibitor measured in this work have been used for evaluating the model. The experimental data along with the calculated methane gas hydrate dissociation conditions in the presence of different concentrations of glycerol up to 700 bar are presented in Figure 5. The model predictions are seen to agree well with the experimental data.

CONCLUSIONS

In this work, we have presented new experimental 3-phase H−L_W−V (Hydrate − Liquid Water− Vapour) equilibrium data for methane clathrate hydrates in the presence of high concentrations of PG and glycerol solutions, generated by a reliable fixed-volume (isochoric), step-heating technique. These data have been used to validate the predictive capabilities of a thermodynamic model presented in this work.

In the thermodynamic model presented here, the Cubic-Plus-Association equation of state is used to model the fluid phases. The hydrate phase is modelled by the solid solution theory of van der Waals and Platteeuw. Good agreement between the model predictions and experimental data is observed, demonstrating the reliability and robustness of the developed model. The CPA EoS is shown to be a very successful model for multi-phase multi-component mixtures containing hydrocarbons, glycols and water.

ACKNOWLEDGMENTS

This work was funded by Petrobras, Statoil and TOTAL, whose support is gratefully acknowledged.

REFERENCES

[1] Chapoy A, Haghighi H, Tohidi B. *A generalized thermodynamic model for predicting the phase behaviour of gas hydrates in reservoir fluids,* Advances in Chemistry Research, Volume 4, Nova Science Publishers, 2010.

[2] Van der Waals JH, Platteeuw JC. *Clathrate solutions*. Adv. Chem. Phys. 1959; 2:1–57.

[3] Tohidi B, Burgass RW, Danesh A, Todd AC, Østergaard KK. *Improving the Accuracy of Gas Hydrate Dissociation Point Measurements*. Ann. N.Y. Acad. Sci. 2000; 912:924-931.

[4] Haghighi H, Chapoy A, Tohidi B. *Experimental and thermodynamic modelling of systems containing water and ethylene-glycol: application to flow assurance and gas processing*. Fluid Phase Equilibr. 2009; 276:24-30.

[5] Haghighi H, Chapoy A., Tohidi B. *Experimental data and modelling methane and water phase equilibria in the presence of single and mixed electrolyte solutions using the CPA equation of state*. J. Oil Gas Sci. Technol. 2009;64(2):141-154.

[6] Haghighi H, Chapoy A, Burgess R, Mazloum S, Tohidi B. *Phase equilibria for petroleum*

reservoir fluids containing water and aqueous methanol solutions: Experimental measurements and modelling using the CPA equation of state. Fluid Phase Equilibr. 2009;278:109–116.

[7] Soave G., *Equilibrium constants from a modified Redlich-Kwong equation of state*, J. Chem. Eng. Sci., 1972;27:1197-1203.

[8] Wertheim M.S., *Thermodynamic perturbation theory of polymerization*, J. Chem. Phys., 1987;87:7323-7331.

[9] Kontogeorgis G.M., Yakoumis I.V., Meijer H., Hendriks E.M., Moorwood T. *Multicomponent Phase Equilibrium Calculations for Water–Methanol–Alkane Mixtures*. Fluid Phase Equilibr. 1999;158:201.

[10] Derawi S., Michelsen M., Kontogeorgis G.M., Stenby, E.H., *Application of the CPA equation of state to glycol/hydrocarbons liquid–liquid equilibria*, Fluid Phase Equilibr. 2003;209:163-184.

[11] Oliveira M.B., Teles A.R.R., Queimada A.J. Couthinho J.A.P. *Phase equilibria of glycerol containing systems and their description with the Cubic-Plus-Association (CPA) Equation of State.* Fluid Phase Equilibr. 2009;280:22–29.

[12] Huang S.H., Radosz M., *Equation of State for Small, Large, Polydisperse and associating molecules*, Ind. Eng. Chem. Res., 1990;29: 2284–2294.

[13] Mathias P.M., Copeman T.W., *Extension of the Peng-Robinson equation of state to polar fluids and fluid mixtures*, Fluid Phase Equilibr., 1983;13:91–108.

[14] Coquelet C.; Chapoy A.; Richon D. Int. J. Thermophys. 2004;25 (1):133-157.

[15] Parrish WR, Prausnitz JM. *Dissociation pressures of gas hydrates formed by gas mixtures*. Ind. Eng. Chem. Process Des. Dev. 1972;11(1):26–35

[16] Anderson FE, Prausnitz JM. *Inhibition of gas hydrates by methanol*. AIChE J. 1986;32(8):1321-1332.

[17] Kihara T. *Virial coefficient and models of molecules in gases*. Rev. Modern Phys. 1953;25(4):831– 843.

[18] McKoy V, Sinanoğlu O. *Theory of dissociation pressures of some gas hydrates*. J. Chem. Physics 1963;38(12):2946-2956.

[19] Tohidi-Kalorazi B. *Gas Hydrate Equilibria in the Presence of Electrolyte Solutions*. Ph.D. Thesis, Heriot-Watt University, 1995.

[20] Holder GD, Corbin G, Papadopoulos KD. *Thermodynamic and molecular properties of gas hydrate from mixtures containing methane, argon and krypton*. Ind. Eng. Chem. Fundam. 1980;19:282-286.

[21] Galvao AC., Francesconi AZ. *Methane and carbon dioxide solubility in 1,2-propylene glycol at temperatures ranging from 303 to 423K and pressures up to 12 MPa*. Fluid Phase Equilibr. 2010; 289:185-190.